 Human Molecular Genetics, 2002, Vol. 11, No. 17 1911–1926

Dysregulation of gene expression in the R6/2 model of polyglutamine disease: parallel changes in muscle and brain

Ruth Luthi-Carter[1], Sarah A. Hanson[1], Andrew D. Strand[2], Donald A. Bergstrom[2], Wanjoo Chun[2], Nikki L. Peters[1], Annette M. Woods[1], Edmond Y. Chan[3], Charles Kooperberg[2], Dimitri Krainc[1], Anne B. Young[1], Stephen J. Tapscott[2] and James M. Olson[2,*]

[1]Center for Aging, Genetics and Neurodegeneration, Massachusetts General Hospital, Charlestown, MA 02129-4404, USA, [2]Fred Hutchinson Cancer Research Center, Seattle WA 98109, USA and [3]Center for Molecular Medicine and Therapeutics, Department of Medical Genetics, University of British Columbia, Vancouver, British Columbia, Canada V5H 4H4.

Received March 12, 2002; Revised and Accepted June 24, 2002

Previous analyses of gene expression in a mouse model of Huntington's disease (R6/2) indicated that an N-terminal fragment of mutant huntingtin causes downregulation of striatal signaling genes and particularly those normally induced by cAMP and retinoic acid. The present study expands the regional and temporal scope of this previous work by assessing whether similar changes occur in other brain regions affected in Huntington's disease and other polyglutamine diseases and by discerning whether gene expression changes precede the appearance of disease signs. Oligonucleotide microarrays were employed to survey the expression of ~11 000 mRNAs in the cerebral cortex, cerebellum and striatum of symptomatic R6/2 mice. The number and nature of gene expression changes were similar among these three regions, influenced as expected by regional differences in baseline gene expression. Time-course studies revealed that mRNA changes could only reliably be detected after 4 weeks of age, coincident with development of early pathologic and behavioral changes in these animals. In addition, we discovered that skeletal muscle is also a target of polyglutamine-related perturbations in gene expression, showing changes in mRNAs that are dysregulated in brain and also muscle-specific mRNAs. The complete dataset is available at www.neumetrix.info.

INTRODUCTION

Huntington's disease is a neurodegenerative disorder caused by a CAG repeat expansion in the *IT15* gene, which encodes a protein known as huntingtin (1–3). Huntingtin is expressed widely throughout the body and central nervous system (4–6). The initiation of the HD process requires the translation of the variable CAG repeat, placing HD into the category of polyglutamine [poly(Q)] diseases (7,8). The etiologic cascade of HD and the other poly(Q) diseases remains unclear.

As limited information can be gathered about a neurodegenerative process from non-invasive *in vivo* procedures and postmortem studies of human cases, the elucidation of poly(Q) pathogenesis relies heavily on disease models. The R6/2 mouse created by Bates and colleagues (9) has thus far been the most widely studied HD model system, and the pathology and phenotypic characteristics of these animals are well documented. R6/2 mice express an N-terminal portion of human huntingtin with a poly(Q) stretch of ~150 under control of the human *IT15* promoter. Interestingly, small N-terminal fragments of huntingtin appear to be generated by proteolysis *in vivo* (10–13), raising the possibility that the effects of such fragments are relevant to human disease.

Behaviorally, R6/2 animals are first distinguished from their wild-type counterparts by a spatial learning deficit [at 3–4 weeks of age (14)]. Attention learning deficits, abnormal performance in motor tests (swimming and high speed rotorod) and reduced long-term potentiation (LTP) appear at 5–6 weeks of age (14–16), followed by the development of a resting tremor, gait disturbances, visual learning deficits and impaired prepulse inhibition at 8–9 weeks of age (14,15). The neurologic status of the animals continues to decline over time, and they die at ~13–15 weeks of age.

Pathologically, neuronal intranuclear inclusions are visible by 3–4 weeks of age in the cortex and by 4–6 weeks of age in the striatum and cerebellum of the R6/2 animal (17,18, and R.L.-C.

*To whom correspondence should be addressed at: Fred Hutchinson Cancer Research Center, D4-100, 1100 Fairview Ave N, Seattle, WA 98109, USA. Tel: +1 2066677955; Fax: +1 2066672917; Email: jolson@fhcrc.org

and A.B.Y., unpublished observations). Although general atrophy of the cortex and striatum has been noted by 12 weeks of age, neither cell loss nor signs of enhanced cell death are detectable at this time point (19). [Signs of dark cell degeneration can be detected only in animals beyond 14 weeks of age, and this occurs only in limited regions of striatum and cortex (19).] The R6/2 mouse is thus a reasonable model in which to study changes of gene expression in the absence of cell loss caused by overt neuronal degeneration. The degree to which R6/2 animals have been characterized, combined with their relatively consistent timeline of biochemical and behavioral changes, provide an opportunity to determine where a particular biochemical change falls within the cascade of their disease process.

Regional specificity is the rule in Huntington's disease, with the striatum and cerebral cortex being affected early in the disease course (20,21). It is not clear whether region-specific effects exist in the R6/2 model, however. In fact, evidence to date suggests that multiple brain regions and peripheral tissues in which the transgene is expressed are subject to poly(Q) toxicity (16,22–24). In this study, we have explored the relative effects of the R6/2 transprotein on gene expression in various brain regions and skeletal muscle. These experiments allow us to address whether changes in steady-state mRNA populations caused by a mutant N-terminal huntingtin fragment show an inherent regional specificity. Further, since the *IT15* (huntingtin) promoter directs the expression of the R6/2 transgene, we were able to examine the extent to which the HD gene promoter might convey regionally restricted effects on gene expression.

In a previous study, we found evidence of specific effects on gene regulation in the striata of R6/2 mice at 6 and 12 weeks of age, representing early and late symptomatic states, respectively (25). These experiments showed the general downregulation of striatal signaling genes and the general upregulation of genes indicative of stress and inflammation. In examining known regulatory mechanisms of the differentially expressed genes, we determined that many of these genes were positively regulated by cAMP, retinoids or interferons. Other studies have also provided strong evidence that transcription may be a major target of poly(Q) disease pathogenesis (26–32).

The current study builds on our previous work in several important ways. To explore the extent to which other tissues are subject to transcriptional perturbation by an expanded poly(Q) protein, we compared poly(Q)- related changes in gene expression in other brain regions and skeletal muscle in R6/2 mice with those observed in striatum. Specifically, we tested whether gene expression changes in R6/2 mice would be more severe in brain tissues affected in HD (striatum and cerebral cortex) than in other tissues (cerebellum and muscle). Also, we assessed the extent of overlap in the mRNAs showing differential expression in one or more regions. Another major aim of our study was to determine where changes in gene expression fall temporally along the continuum of well-characterized behavioral and pathologic signs of poly(Q) disease observed in R6/2 animals. To address this question, we used a combination of microarray and northern analyses to assess the timing of mRNA changes before and throughout the development of pathologic and behavioral disease parameters.

These studies demonstrate that the N-terminal huntingtin fragment can have dramatic effects on gene expression, and suggest that no regional selectivity of this effect is imparted by the *IT15* promoter or N-terminal huntingtin polypeptide sequences. Further, mRNA changes appear early in the disease process in R6/2 mice [approximately coincident with changes in LTP (16)], but do not precede the formation of neuronal inclusions or the development of spatial learning deficits.

RESULTS

Regional gene expression profiles in control and R6/2 mouse brain

R6/2 mice develop learning, motor and coordination deficits suggesting that multiple brain regions are adversely affected by the poly(Q) expansion (9,14,15). In order to place transcriptional changes in each brain region into the appropriate context, we first established which genes were present in each tissue. Figure 1A shows the number of genes that were called 'Present' (detectable) by Affymetrix GeneChip software (version 4.0) in at least 50% of the samples assayed. Nearly half of all probes on the arrays detected transcripts in all three regions by these criteria. Of the mRNAs that were preferentially detected in one brain region, many are consistent with *in situ* hybridization and northern analysis results reported in the literature. The complete region-specific data set is provided in the supplemental datafile "Region_Specific_Data.xls" at www.neumetrix.info. A similar list of genes that meet the criteria of being called 'Present' at a threshold of 75% is also provided at this site. These brain region-specific transcript expression maps provide information for a broad array of uses, including the generation of mice with region-specific transgene expression. It also provides information about probes that do not reliably detect particular mRNAs, providing a basis for interpreting negative results.

To better understand the regional scope of transcriptional dysregulation in this animal model, we compared gene expression profiles from 12-week R6/2 striatum, cortex and cerebellum with those of wild-type controls. The error model described in (33) revealed that a small fraction (1–2% at $P < 0.001$) of assayed transcripts were differentially detected in each brain region (Table 1). In each case, the predicted false-discovery rate was less than 10% of the number of mRNAs that met the $P < 0.001$ threshold at this age (Table 1). Very few transcripts (only 34) were differentially detected in all three brain regions of R6/2 compared with wild-type mice (Fig. 1B). Transcripts that were differentially detected in three of three regions or in two of three regions are shown in Figure 2A. Selected mRNAs that were differentially detected in only cortex or cerebellum are listed in Figure 2B, and the complete dataset is available at www.neumetrix.info.

The Mu11K GeneChips used for this study assay the expression of ~5000 more mRNAs than those used in a previous analysis (Mu6500) (25); therefore, we obtained additional information on striatal gene expression. Also, some changes in gene expression in R6/2 animals were observed uniquely in cerebral cortex and/or cerebellum (whereas no changes in striatal expression were detected, often because these particular mRNAs were absent or of low abundance in

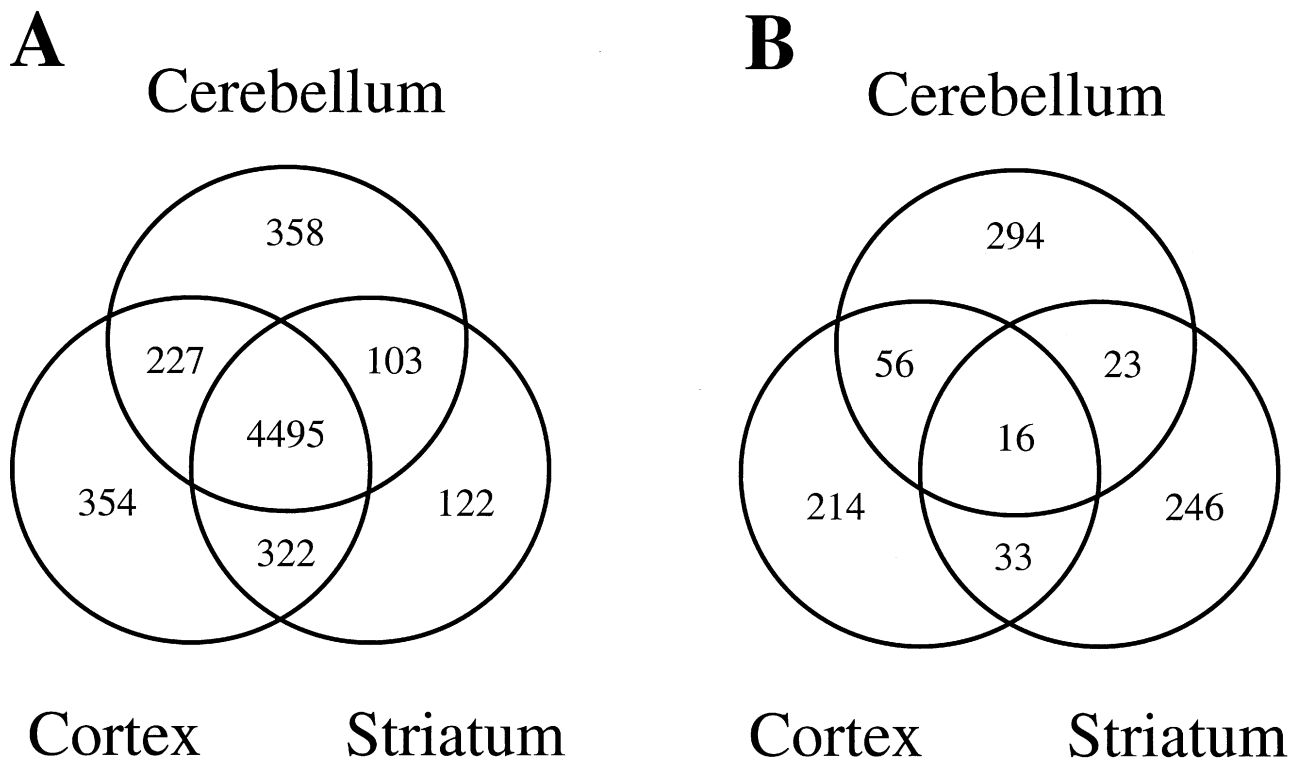

Figure 1. Summary of mRNA detection and changes in cerebellum, cerebral cortex and striatum. (**A**) Venn diagram showing the number of microarray probes that detected a signal in at least 50% of samples from the specified brain regions. The total number of probes on the arrays was 13 179. (**B**) The number of mRNAs that were differentially detected in brain regions of 12-week old R6/2 mice compared with littermate controls using a threshold of $P < 0.01$. The predicted number of false discoveries has been subtracted, so that the diagram shows only the predicted number of true-positive discoveries for each brain region at this threshold.

Table 1. The number of gene expression changes in R6/2 brain versus control at $P < 0.001$

Tissue	Striatum				Cerebellum	Cortex		
Age (weeks)	2	4	6	12	12	2	6	12
Replicates	2	2	2	2	2	3	3	3
$P < 0.001$	7	1	29	147	183	25	62	182
1−FDR	0.00	0.00	0.55	0.91	0.93	0.48	0.79	0.93
Confirmed/examined	0 of 2	ND	3 of 3	10 of 11	14 of 17	0 of 6	3 of 3	13 of 13

The number of mRNAs that were differentially detected using the error model method described by Strand and colleagues is shown in the row labeled, '$P < 0.001$' (33). The row labeled, '1−FDR' reports the calculated fraction of true-positive differences for each condition. The row labeled 'Confirmed/examined' shows the number of mRNA changes that were differentially detected by other methods (e.g. northern analysis and RT–PCR) at $P < 0.05$. Not included in this row were 7 out of 7 proteins that were differentially detected by western analysis in the same direction as the corresponding mRNAs were altered by microarray analysis. ND, no data.

striatum). Since more mRNAs and additional brain regions were examined in the present study, many novel changes were detected. Data for striatal mRNAs assayed on both Mu11K and Mu6500 arrays (i.e. those examined in both the previous and present analyses) showed good concordance between studies.

As seen in our previous analysis of R6/2 striatum, mRNAs that were decreased in cerebral cortex and cerebellum were largely comprised of those that encode neuropeptides [e.g. preprosomatostatin, enkephalin, neuropeptide Y, prodynorphin and cholecystokinin (CCK)] and other proteins involved in neurotransmission [e.g. the GABA receptor δ subunit and protein kinase C (PKC)] and proteins involved in ion regulation (the ryanodine receptor and potassium channel proteins). Newly apparent were genes related to growth factor signal transduction [e.g. brain-derived neurotrophic factor (BDNF), bone morphogenetic protein 1, the growth factor-inducible immediate early gene 3CH134 and insulin-like growth factor-binding protein 5 (IGFBP5)]. Messenger RNAs that were increased in multiple brain regions of R6/2 mice were consistent with a cellular response to stress induced by the poly(Q)-containing transprotein (e.g. the proteasome PA28 subunit and DNA-repair enzymes). Newly appreciated mRNA increases included those encoding RNA polymerases and tRNA synthetic enzymes. A subset of the differentially expressed mRNAs was further assessed by northern analysis (Fig. 3).

Figure 2A mRNAs that are changed in more than one R6/2 brain region

GenBank ID	Description	R6/2 Q150 vs wt striatum 12 week		R6/2 Q150 vs wt cortex 12 week		R6/2 Q150 vs wt cerebellum 12 week	
U29762	albumin gene D-Box binding protein		-5.8		-10		-4.4
AA221393	calcium-transporting ATPase sarcoplasmic reticulum type*		-2.0		-2		-2.1
M13227	enkephalin		-4.1		-3		-1.8
M22326	growth factor-induced protein (zif/268)		-2.1		-2		-1.8
X16995	N10 gene for a nuclear hormonal binding receptor.		-2.1		-3		-2.9
X70398	P311		-2.7		-3		-1.3
X17320	pcp-4 gene for putative brain specific antigen.		-3.5		-2		-1.9
AA172864	platelet glycoprotein 1B beta*		-1.9		-2		-1.7
X51468	preprosomatostatin gene		-1.9		-4		-5.0
X83932	ryanodine receptor type 1.		-2.7		-5		-2.1
D87909	PA28 alpha subunit		1.8		1.5		2.1
AF026489	beta III spectrin (Spnb3)		-1.7		-1		-2.1
V00722	beta-1-globin.		-1.9		-0		-1.9
L07264	heparin-binding EGF-like growth factor		-1.7		-1		-1.5
U95610	nimA-related kinase 2 (Nek2)		-1.0		0.4		-1.7
X15373	P400		-2.8		-2		-3.7
U96634	p85SPR		-3.4		-2		-3.1
AA106166	elongation factor 2*		3.8		0.7		1.7
AA071776	glucose-6-phosphate isomerase*		1.8		1.5		2.5
AA221937	LY6-B antigen*		1.8		1.4		14.0
D78255	PAP-1		2.9		0.8		1.6
W42234	Xeroderma Pigmentsum DNA-repair XP-E*		1.9		-1		2.2
AA020101	brain protein H5*		-1.9		-2		-1.4
AA289338	cAMP-regulated phosphoprotein*		-5.1		-3		-1.2
M13227	enkephalin mRNA		-4.2		-3		-1.5
U92565	fractalkine		-2.2		-2		1.3
U92565	fractalkine		-2.5		-2		-0.3
W10739	G0/G1 switch regulatory protein 8*		-2.9		-2		0.1
M60596	GABA-A receptor delta-subunit		-3.9		-6		-1.6
W54905	hippocalcin, neuron specific calcium binding*		-2.5		-2		-1.2
AA017811	neurogranin (protein kinase C substrate)*		-2.1		-2		-0.2
W70782	neuropeptide Y*		-1.9		-3		1.4
X51468	preprosomatostatin gene.		-2.0		-4		-1.6
D38613	presynaptic protein 921-L		-1.7		-2		-1.4
AF026537	prodynorphin mRNA		-5.9		-4		0.3
X53532	protein kinase C beta-II.		-2.9		-2		-1.3
AA116737	protein phosphatase inhbitor 1*		-2.6		-2		-0.2
U06483	telencephalin precursor		-2.2		-2		-1.1
L39123	apolipoprotein D		1.9		1.8		1.6
X82648	apolipoprotein D.		1.6		1.8		1.3
W15824	DNA-directed RNA polymerases I & III*		3.4		2.6		0.1
Z22593	fibrillarin		1.9		1.6		1.3
M32599	glyceraldehyde-3-phosphate dehydrogenase		1.8		4.7		-0.9
U39473	histidyl-tRNA synthetase		1.8		1.4		-0.1
AA034761	tRNA processing protein SEN3*		2.2		1.6		1.2
X51438	vimentin.		2.3		1.9		-1.1
W77701	acylphosphatase*		-1.3		-2		-1.9
X98014	alpha-2,8-sialyltransferase.		-0.9		-2		-4.2
L24755	bone morphogenetic protein 1 (BMP-1)		-1.6		-3		-2.5
X55573	brain-derived neurotrophic factor		-1.4		-2		-3.2
V00727	c-fos oncogene.		-0.1		-5		-26.7
W64587	calcium-transporting ATPase sarcoplasmic reticulum type*		-1.8		-2		-2.2
U37091	carbonic anhydrase IV gene		-0.1		-2		-1.9
AF016697	chemokine receptor gene		-1.8		-2		-3.2
X59520	cholecystokinin		0.0		-2		-18.0
X59520	cholecystokinin		2.4		-2		-28.6
AA000227	diacylglycerol kinase (retinal degenration A protein)*		0.3		-2		-2.4
AA059718	DNA polymerase beta*		-0.2		-2		-1.9
X61940	growth factor-inducible immediate early gene (3CH134).		-1.5		-3		-2.6
L12447	insulin-like growth factor binding protein 5 (IGFBP5)		-1.5		-2		-3.0
Y00305	MBK1 mRNA for brain potassium channel protein-1.		-1.5		-2		-2.0
U47543	NGFI-A binding protein 2 (NAB2)		-1.8		-2		-9.3
U86783	Nurr1, steroid/thyroid hormone orphan nuclear receptor		-0.2		-3		-11.4
X59382	parvalbumin gene exon 5 5-part		-1.1		-2		-1.8
X67141	parvalbumin.		-1.2		-2		-1.9
AF022992	Rigui		-3.7		-5		-1.9
AF022992	Rigui		-1.6		-2		-2.1
W54638	sodium/potassium ATPase alpha-1*		-1.3		-2		-2.0
AF026489	spectrin, beta III		-1.8		-2		-2.5
AF010305	Stra13 mRNA		0.1		-3		-2.5
U61751	vesicle-associated membrane protein VAMP-1		2.4		-4		-3.8
U12473	Balb/c conserved helix-loop-helix ubiquitous kinase (CHUK)		1.3		2.1		1.9
AA089333	cathepsin*		1.9		1.6		3.7
U42385	fibroblast growth factor inducible gene 16 (FIN16)		1.5		2.7		2.8
M18184	lymphocyte differentiation antigen (Ly-6.2)		-0.2		1.6		2.8
U49351	lysosomal alpha-glucosidase		1.3		1.5		1.8
U71202	rin		1.6		1.4		1.8
M12130	RNA polymerase II large subunit gene		3.6		2.9		20.1
U37500	RNA polymerase II largest subunit (RPB1)		1.7		1.9		2.9
L32973	thymidylate kinase homologue		1.7		1.5		2.3

[a] sequence homologous to named gene
[b] blast search reveals no named homolog

Figure 2. Altered mRNAs in R6/2 mouse brain compared with control. (**A**) mRNAs that were significantly different in two or more regions of R6/2 brain. GenBank number and gene description are on the left. For each brain region, independent replicates are shown as columns of red (increased in R6/2 compared with control) and green (decreased in R6/2). Brighter colors represent increased confidence (e.g. net probe pair changes >35% are represented by the brightest colors, then 25–35% dimmer, then >15–25% dimmer, then black for <15%). The rightmost column for each brain region is the mean fold change in R6/2 compared with control as calculated by Affymetrix GeneChip software version 4.0. *P*-values are those calculated from the array data as in (33). Expressed sequence tags (ESTs) are not shown. ESTs that were decreased in at least two regions were R75030, AA408337, AA288448, AA607353, N28171, AA275198, AA184116, AA028770, AA217531, AA673405, AA144045, AA271049, AA028770, AA166452, W63829, AA267683, AA028280, AA163244 and AA271603. ESTs that were increased in at least two regions were W12941, AA575675, AA199023, AA209580, AA217493, AA217411, Z31269, C77662, AA638408, AA407204, AA116735, AA546670, AA611940, and AA616578. (**B**) Selected mRNAs that were differentially detected in one region (cortex or cerebellum) of R6/2 brain. Green bars represent mRNAs that were decreased at $P < 0.001$ and red represents increases at the same threshold. The complete list of mRNAs that were changed in each brain region is posted at supplemental data (www.neumetrix.info).

Figure 2B Select changes unique to cortex or cerebellum

Cerebral Cortex

Genbank	Description
X83202	11beta-hydroxysteroid dehydrogenase/carbonyl reductase
W13586	atrial/fetal isoform myosin alkali light chain (MALC)
U51908	brain neurotensin receptor
X14836	calmodulin kinase II
AA124698	discs large-1 tumor suppressor*
U68058	frezzled
W53351	fructose-bisphosphate aldolase C*
Z36270	GC Binding Protein
Y12257	glutamic acid decarboxylase 67 kD
M13366	glycerophosphate dehydrogenase
U69262	matrilin-2 precursor
AJ001118	monoglyceride lipase.
X54149	MyD118, a myeloid differentiation primary response gene
M19436	myosin alkali light chain (Myla, atrial/fetal)
AF011644	oral tumor suppressor homolog (Doc-1)
AF011644	oral tumor suppressor homolog (Doc-1)
AF011644	oral tumor suppressor homolog (Doc-1)
D14423	preprotachykinin B
AA059662	protease DO precursor*
U24703	reelin
U04268	Sca-2 precursor
X85991	semaphorin B.
W12919	sodium/potassium ATPase alpha-1*
AA105755	sodium/potassium ATPase alpha-1*
AA117973	sodium/potassium ATPase alpha-1*
AA063844	sodium/potassium ATPase alpha-3*
X68951	somatostatin receptor
M29793	troponin C, slow/cardiac
U76007	zinc transporter ZnT-3
AA269806	histone H2A.X*
M63650	M-twist
AA510387	ribose-phosphaate pyrophosphokinase I*
AA072842	sodium and chloride -dependent transporter NTT73*
U62297	transcription factor NF-YC subunit
X87617	Ulip protein

Cerebellum

Genbank	Description
X78197	AP-2 beta
W65178	bone morphogenetic protein 1 (BMP-1)*
AA008502	brain neuron cytoplasmic protein 1*
AA059527	brain neuron cytoplasmic protein 2*
D13266	glutamate receptor channel delta 2 subunit
D21165	neural visinin-like Ca2+-binding protein type 1 (NVP-1)
AA111277	neural visinin-like protein 3*
AA105135	p53 binding protein*
X67141	parvalbumin.
M69042	protein kinase C delta
X60304	protein kinase C-delta.
L28035	protein kinase C-gamma
M90388	protein tyrosine phosphatase (70zpep)
D31898	protein tyrosine phosphatase, PTPBR7
AA444931	SNF1-related kinase*
AA444931	SNF1-related kinase*
M21285	stearoyl-CoA desaturase gene
X03151	Thy-1 antigen.
W21013	brain specific homeobox*
ET63241	Caspase-3 (Lice)
AA255186	cathepsin precursor*
AA146437	cathepsin precursor*
U54903	cysteine protease (Lice)
AF012129	DNA methyltransferase (Dnmt2)
U72519	Ena-VASP like protein (Evl)
U11860	G protein coupled inward rectifier K+ channel 3
K01347	glial fibrillary acidic protein (GFAP)
W47726	glycogen synthase kinase-3 alpha*
AA120109	interferon-induced protein 6-16*
W09701	JUN-C, transcription factor component of AP-1*
W29356	JUN-D transcription factor
M60474	myristoylated alanine-rich C-kinase substrate (MARCKS)
AA072252	phosphofructokinase I*
D38218	ryanodine receptor, RyR3
AA066097	TAFII31, TBP-associated factor*

* sequence similar to named gene

Figure 2 *continued.*

Time course of gene expression changes in R6/2 animals

We extended our array analyses to 2-, 4- and 6-week striatum and 2- and 6-week cerebral cortex. Application of the error model (33) revealed that the numbers of mRNAs detected at the 2- and 4-week time points were within the range of predicted false-positives. We conclude that when using this technology in homogenate samples of striatum and cortex, no transcription dysregulation can reliably be detected in the 2- and 4-week and samples (Table 1). To assess whether the GeneChips simply lacked sensitivity to detect changes in these samples, we conducted time-course studies by northern analysis for six mRNAs that were changed in R6/2 striatum at the 6- or 12-week time points. None of these mRNAs was differentially detected in 2- or 4-week samples by phospoimage analysis after normalization for sample loading. In 6-, 8-, 10- and 12-week samples, northern analysis confirmed the changes detected by microarray (Fig. 4A and 5). We similarly extended microarray findings in cerebellum and cerebral cortex by conducting a time-course study using northern analyses. As in striatum, gene expression changes in these regions were first detected at 6 weeks, and uniformly confirmed microarray-based findings (Fig. 4B, 4C and 5).

Changes in the expression of Sp transcription factor-regulated genes

For mRNAs that were differentially detected in R6/2 mice compared with controls, we analyzed the corresponding promoter sequences for known transcription factor motifs. We found that all of the promoters that had been characterized contained putative binding sites for Sp transcription factors within 500 bp of the transcription start site (Table 2). Table 2 lists genes of which the promoter has been formally studied and in which an Sp site was present. Consistent with our previous study, we again noted many retinoid- and cAMP-responsive genes among those downregulated in R6/2 brain.

Comparisons of RNA and corresponding protein levels in R6/2 brain

In a recent study, mRNA levels detected by microarray analysis showed limited correlation with protein levels detected by mass spectrometry (34). To determine whether protein levels determined by western analysis corresponded to RNA levels in R6/2 mice, we conducted western analysis of brain homogenates from R6/2 and control mice at 8 and 12 weeks of age. Protein levels were altered in the same direction as mRNA levels in all but one case (RNA polymerase II in cerebellum, see below). In addition, protein levels were more uniformly changed across the three regions of brain that were assayed (cerebellum, cerebral cortex and striatum) than were mRNA levels. By western analysis, calbindin, glutamic acid decarboxylase and neurofilament medium chain were decreased in all three brain regions examined, and excitatory amino acid transporter EAAT4, c-kit, and neuron-specific enolase (NSE) were decreased in selected brain regions. Also, glial fibrillary acidic protein (GFAP) was increased in the cerebellum and cerebral cortex (Fig. 6). These results confirmed that changes in mRNA

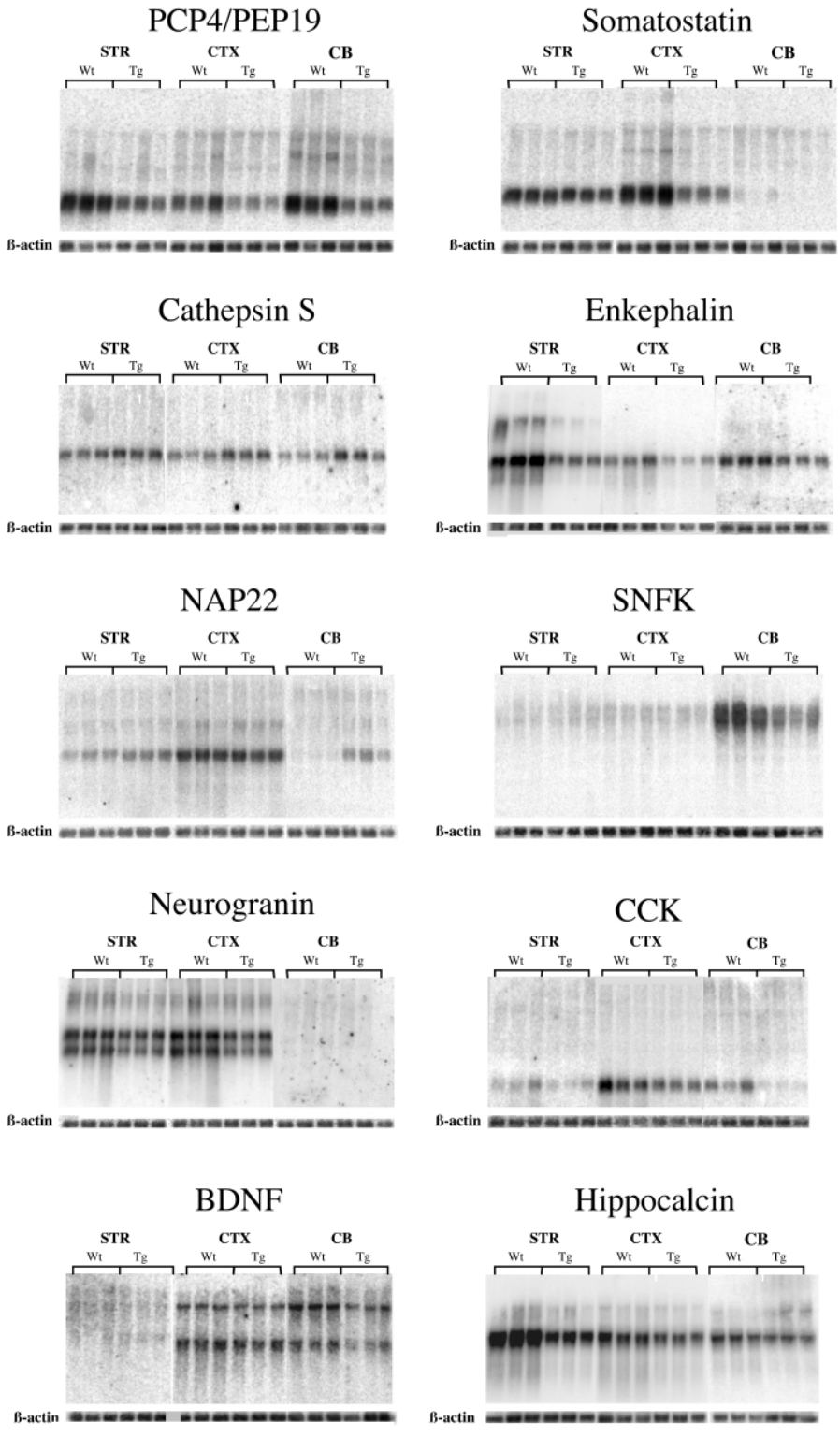

Figure 3. Northern analyses of mRNA showing differential expression by microarray analysis. Blots containing 2 µg of total mRNA from individual R6/2 (Tg) or wild-type (Wt) animals was probed with sequence-confirmed cDNA probes (see Materials and Methods). Both regionally distinct variations in basal gene expression and differential detection of changes in R6/2 animals supported the microarray results in all cases. PCP4/PEP19 Purkinje cell protein 4/brain-specific polypeptide 19; NAP22, neuronal acidic protein-22; SNFK, Snf-1-related kinase; CCK, cholecystokinin; BDNF, brain-derived neurotrophic factor. Quantitation of the R6/2 data as mean percentage of control ±SEM of three wild-type and three transgenic samples: PCP4/PEP19: striatum (STR) 22.7 ±1.6, cortex (CTX) 41.0 ±1.0, cerebellum (CB) 25.0 ±1.7; somatostatin: STR 59.2 ±4.5, CTX 24.8 ±3.7, CB 46.1 ±11.7; cathepsin S: STR 175.8 ±14.4, CTX 134.6 ±6.8, CB 167.1 ±37.4; enkephalin: STR 30.6 ±2.3, CTX 56.8 ±4.6, CB 60.1 ±27.7; NAP22: STR 111.8 ±6.3, CTX 66.1 ±1.9, CB 478.0 ±23.6; SNFK: STR 128.9 ±5.8, CTX 113.1 ±7.3, CB 50.9 ±8.6; neurogranin: STR 48.7 ±1.5, CTX 36.2 ±1.1, CB 672.0 ±553.1; CCK: STR 55.4 ±16.4, CTX 52.6 ±3.0, CB 10.5 ±8.7; BDNF: STR 47.1 ±3.7, CTX 90.1 ±5.3, CB 58.4 ±5.6; hippocalcin: STR 43.6 ±3.8, CTX 56.3 ±1.1, CB 43.9 ±0.4.

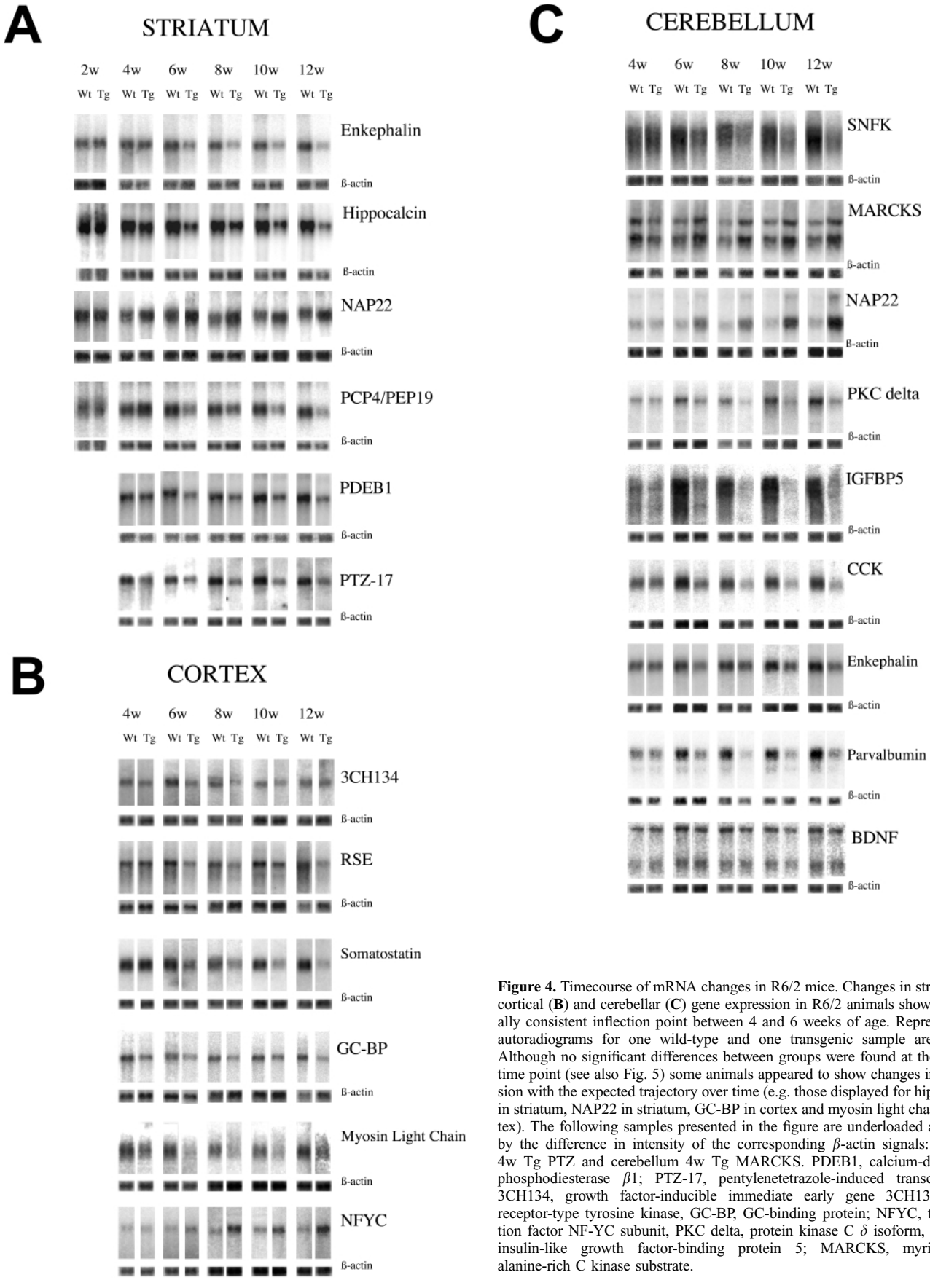

Figure 4. Timecourse of mRNA changes in R6/2 mice. Changes in striatal (**A**), cortical (**B**) and cerebellar (**C**) gene expression in R6/2 animals show a generally consistent inflection point between 4 and 6 weeks of age. Representative autoradiograms for one wild-type and one transgenic sample are shown. Although no significant differences between groups were found at the 4-week time point (see also Fig. 5) some animals appeared to show changes in expression with the expected trajectory over time (e.g. those displayed for hippocalcin in striatum, NAP22 in striatum, GC-BP in cortex and myosin light chain in cortex). The following samples presented in the figure are underloaded as shown by the difference in intensity of the corresponding β-actin signals: striatum 4w Tg PTZ and cerebellum 4w Tg MARCKS. PDEB1, calcium-dependent phosphodiesterase β1; PTZ-17, pentylenetetrazole-induced transcript 17; 3CH134, growth factor-inducible immediate early gene 3CH134; RSE, receptor-type tyrosine kinase, GC-BP, GC-binding protein; NFYC, transcription factor NF-YC subunit, PKC delta, protein kinase C δ isoform, IGFBP5, insulin-like growth factor-binding protein 5; MARCKS, myristoylated alanine-rich C kinase substrate.

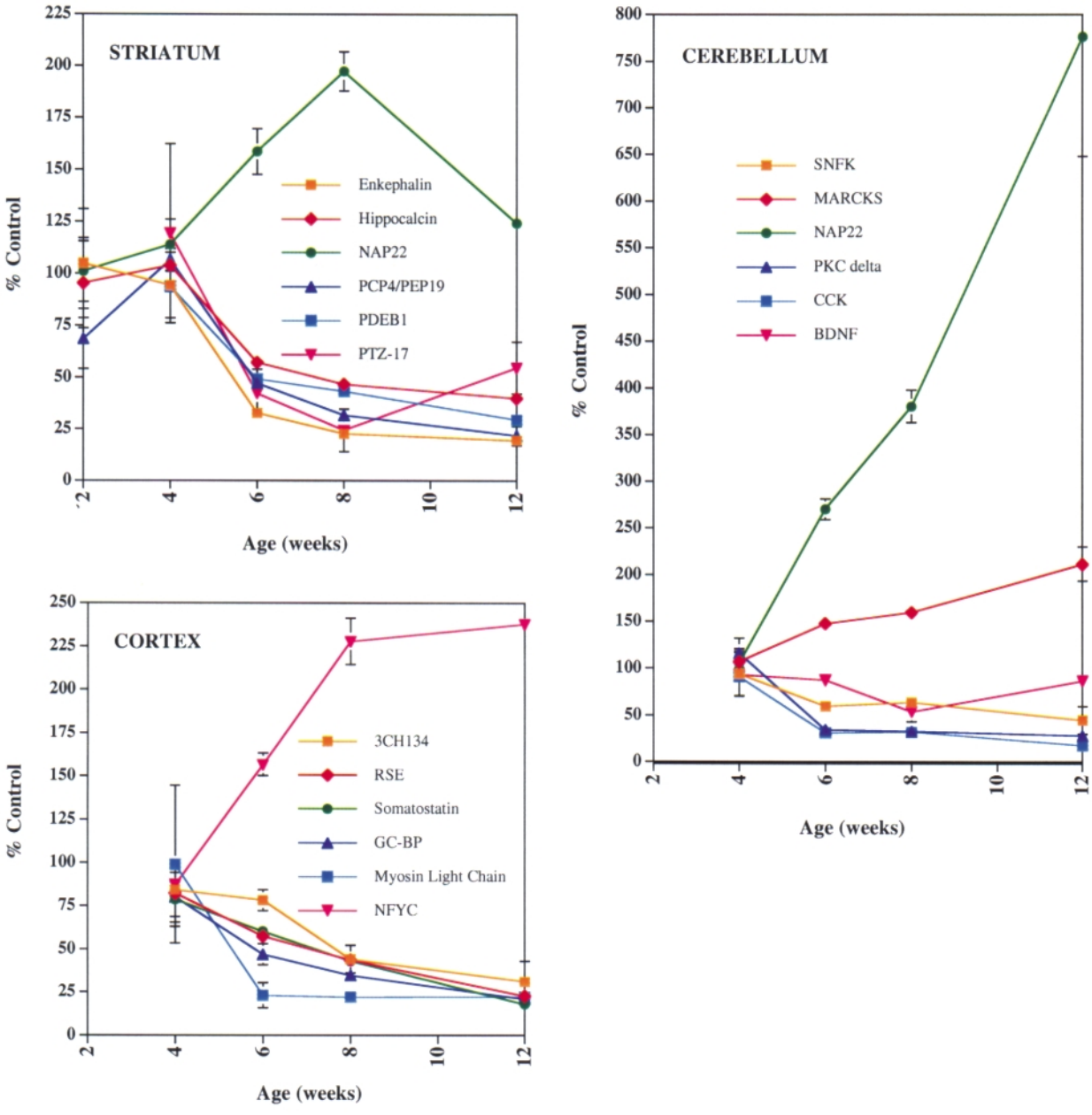

Figure 5. Gene expression changes over time in R6/2 animals. Densitometric analyses of the northern blots shown in Figure 4 were graphed. Each point represents the percentage control ± SEM for three or four R6/2 animals relative to the same number of wild-type animals. Where error bars are not shown, they are contained within the area of the symbol.

levels predicted corresponding changes in protein levels in this model system. They also confirm that changes in gene expression in a particular brain area may significantly affect protein levels, and thus neuronal function, in other regions to which it projects.

RNA polymerase II large subunit (RPIILS) was increased by microarray analysis in all three brain regions of R6/2 mice at 12 weeks compared with controls. Because this molecule plays a critical role in transcription, we conducted further studies of its expression. Northern analysis confirmed the microarray results in all three brain regions (Fig. 7A). In addition, western analysis confirmed that RPIILS protein levels were increased in striatum and cerebral cortex of R6/2 mice (Fig. 7B). The same blots showed that RPIILS protein levels were *decreased* in R6/2 cerebellum compared with wild-type, despite *opposite* findings for mRNA levels. We also assessed whether RPIILS protein is sequestered into poly(Q) aggregates. Indirect immunofluorescence microscopy revealed the presence of RPIILS in both nuclear and cytoplasmic aggregates of an SY5Y neuroblastoma cell line that overexpresses an expanded repeat huntingtin fragment (35). RPIILS co-localized with aggregates in the majority, but not all, of the cells that contained aggregates. The

Table 2. Genes that contain Sp1 response elements in the proximal promoter region

DARPP[A]	α-Actin[Z]
Neurogranin[B]	Calmodulin kinase II[AA]
SEZ-6[C]	Gadd45[BB]
GABA$_A$ δ[D]	Bone morphogenetic protein[CC]
Zif/268[E]	Reelin[DD]
Hippocalcin[F]	Prodynorphin[EE]
ATP synthase A chain[G]	Heavy-chain variable-region antibody[FF]
Ryanodine receptor 1[H]	Carbonic anhydrase[GG]
Creatine kinase B[I]	Cholecystokinin[HH]
Atrial myosin alkali light chain[J]	NURR1[II]
Brain fatty acid-binding protein[K]	Protein kinase Cr[JJ]
Glutamic acid decarboxylase[L]	Insulin-like growth factor binding protein 5[KK]
Preprosomatostatin gene[M]	Calcium-activated potassium channel[LL]
Neuropeptide Y[N]	Id-2[MM]
Glycerophosphate dehydrogenase[O]	Thy-1[NN]
c-Fos[P]	βII spectrin[OO]
Sodium/potassium-transporting ATPase[Q]	14-3-3 η[PP]
Cardiac slow-twitch troponin C[R]	β1-Globin[QQ]
FISP-12 protein[S]	Parvalbumin[RR]
Chemokine receptor[T]	α-2,8-sialyltransferase[SS]
Enkephalin[U]	BDNF gene[TT]
Middle-molecular-mass neurofilament protein[V]	δ-Aminolevulinate dehydratase[UU]
Collagen α1 (VI)[W]	Ubiquitin carboxyl-terminal hydrolase[VV]
T-cell receptor[X]	D2 dopamine receptor [WW]
Rigui[Y]	

The proximal promoter regions for all genes that were altered in R6/2 striatum, cerebellum or cerebral cortex at $P < 0.001$ were analyzed for transcription factor response elements. Promoter sequences were published for approximately 15% of genes that met this criterion. Of these, 100% contained Sp response elements within the proximal 500 bp of the promoter. Manuscripts that report promoter sequence, electrophoretic mobility shift assays, and/or reporter assays are referenced in the supplemental data (www.neumetrix.info). These references correspond to the superscript letters that follow each gene name in the table. Of 4000 mRNAs called present but not differentially expressed between R6/2 animals and controls, a random sampling of approximately 200 yielded 20 characterized promoters, of which 14 (70%) contained Sp response elements by the same criteria. Thus, the percentage of promoters in the differentially expressed genes containing Sp1 sites was higher than predicted by chance alone.

presence of RPIILS in aggregates was not sufficient to deplete the cells of normal, diffuse nuclear protein, as shown in Figure 7C. Additional studies will be required to learn whether sequestration of the RNA polymerase II large subunit in *in vivo* models of HD or in HD patient samples is sufficient to influence transcription of key neuronal genes.

mRNA changes in muscle of R6/2 compared with control mice

There is evidence that mutant huntingtin may have detrimental effects on skeletal muscle (37), and that R6/2 mice have poly(Q) aggregate pathology in this tissue (22). Further, recent reports indicate that expanded poly(Q) aggregates sequester histone acetyltransferases and other transcriptional proteins in brain and in cultured cells (26–29). Based on these results, we predicted that huntingtin would alter gene expression in muscle as well as in brain. We compared gene expression profiles of muscle from 12-week-old R6/2 mice with those of age-matched controls. As seen in brain, ~2% of mRNAs assessed were differentially detected between R6/2 and control muscle and more mRNAs were decreased than increased (Table 3 and neumetrix.info supplemental data). Also as in brain, mRNAs that were increased in muscle were consistent with a cellular stress response to the expanded poly(Q) transprotein (e.g. ubiquitin-conjugating enzymes and multiple DNA-repair enzymes). Messenger RNAs that were decreased in R6/2 compared with control muscle included markers of terminal muscle differentiation (e.g. myoD, actin, myosin light chain and troponin), mRNAs that encode metabolic enzymes (e.g. creatine kinase, enolase and aldolase) and mRNAs that encode signal transduction molecules (e.g. phosphatidylinositol glycan, cAMP-specific phosphodiesterase and Neu-associated kinase).

DISCUSSION

The R6/2 transgenic mouse is the most widely used model of Huntington's disease. In this study, we demonstrate that R6/2 mice have reproducible and widespread gene expression changes in brain and muscle. In 12-week-old R6/2 mice, the *number* and *magnitude* of mRNA changes caused by the expanded htt exon 1 transprotein were similar in all three brain regions examined. These results indicate that the mutant N-terminal huntingtin fragment carried in these mice conveys no inherent regional selectivity, at least at the level of gene expression. Likewise, these results suggest that poly(Q) effects on gene expression in HD are not regionally selective by virtue of the *IT15* promoter, which also directs the expression of the R6/2 transprotein. Because the transprotein expressed by R6/2 mice comprises only a small portion of the full-length amino acid sequence of huntingtin, they are sometimes considered to be a general poly(Q) disease model rather than a model specific for HD. Considered as such, it is possible that many of the gene expression effects observed in R6/2 mice are generalizable to other poly(Q) diseases. We address general poly(Q) effects in a companion paper (38).

The *specific mRNA changes* that were detected were disproportionately high in single regions compared with the region-selective transcript expression maps (compare Figs. 1A and B). We believe that the latter is due to the fact that some gene expression changes remain below the level of sensitivity of the microarray analysis. This is based on a higher rate of detection of changes across multiple brain regions in northern analyses when the same mRNAs were differentially detected in only one or two of the brain regions by microarray. As shown in other studies (33,38,39), it is possible that some of these gene expression changes could be detected through the use of additional replicates.

Gene expression changes prior to 6 weeks of age were not reliably detected by microarray or northern analyses of R6/2 mice. Because gene expression changes were reliably detected within 24–48 hours in yeast cultures and mammalian cell lines that overexpress mutant poly(Q)-encoding transgenes (31,40,41), it is possible that transcriptional changes in young R6/2 mice simply fall below the level of detection. Explanations include asynchronous gene expression changes among subsets of cells in homogenate samples, homeostatic correction of mRNA levels and changes that are very small in

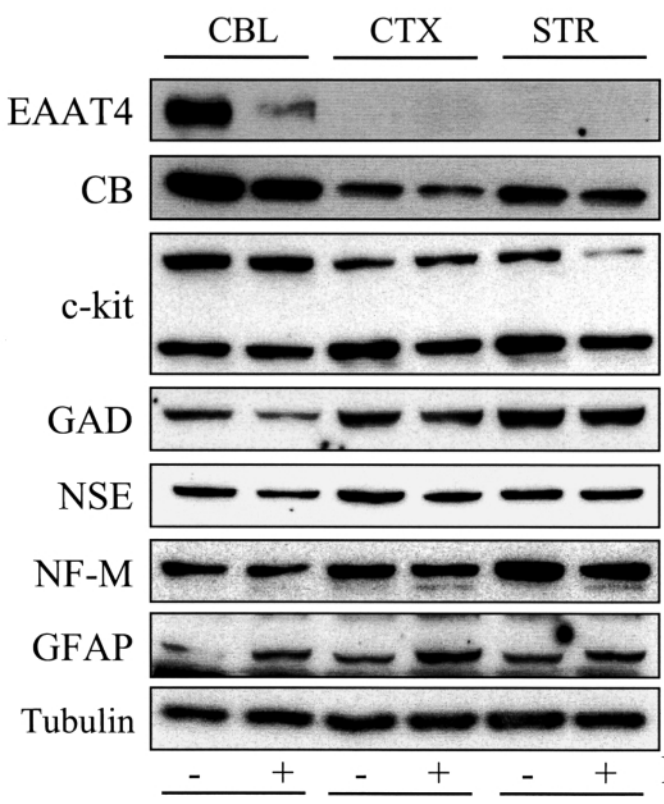

Ratio (%): HD+/HD-

CBL	CTX	STR
18.2	-	-
65.3	64.7	74.1
93.1	97.1	26.2
88.4	68.3	88.4
54.5	78.3	83.4
70.6	66.3	95.4
79.8	81.2	83.6
251.2	178.2	111.2

Figure 6. Western analysis of proteins encoded by genes that were differentially detected in one or more brain regions of R6/2. Western analysis demonstrated, for all proteins tested, that mRNA changes resulted in corresponding protein level changes. Left panel: western blots of excitatory amino acid transporter 4 (EAAT4), calbindin (CB), c-kit, glutamic acid decarboxylase (GAD), neuron-specific enolase (NSE), medium-chain neurofilament (NF-M), and glial fibrillary acidic protein (GFAP) on specimens from cerebellum (CBL), cerebral cortex (CTX) and striatum (STR) of R6/2 (+HD) and wild-type (−HD) mice. Tubulin is shown as a loading control. Right panel: quantitative values for western blots on left.

magnitude. Alternatively, gene expression changes may truly occur later than other disease signs in these animals, which may differ from the cell lines because of a lower transgene dose.

One common pathologic feature of poly(Q) diseases is the formation of multimolecular aggregates that contain the disease protein (42,43). Recently, it has been shown that transcription factor proteins can be recruited away from their normal subcellular compartments and into these aggregates (26–29, 44,45). One consequence of such recruitment may be loss of transcriptional regulation normally controlled by these specific transcription factors (46–50). In this study, we demonstrated for the first time that the RNA polymerase II large subunit co-localizes with aggregates in a cellular model of poly(Q) disease. Future studies are indicated to establish whether an abnormal RPIILS protein interaction is responsible for some of the gene expression changes described in this study. It will also be important to determine whether poly(Q)-containing proteins interact directly with RPIILS or whether the latter is sequestered by virtue of its interaction with other transcriptional proteins that are sequestered. Consistent with data showing sequestration of transcriptional proteins by intranuclear inclusions, gene expression changes become robust in R6/2 brain shortly after large neuronal aggregates form. On the other hand, inclusions form earlier in the cerebral cortex (at 3–4 weeks) than in the striatum or cerebellum (4–6 weeks), yet mRNA changes appear at approximately the same time in all three regions (4–6 weeks), suggesting that gene expression changes could arise from an independent process, such as soluble protein–protein interactions (32). Given the limited time resolution of the present data and the heterogeneous formation of inclusions in the affected regions during this early period of disease, future studies will be required to define more precisely the relationship between aggregate formation and changes in gene expression.

Our data are also consistent with the hypothesis that Sp1-mediated gene regulation may be altered by mutant huntingtin (32,51). We have recently shown that Sp1 interacts with huntingtin directly, and that mutant huntingtin has a higher affinity for this transcriptional regulator than does the wild-type protein (32). Further, we have shown that Sp1-dependent transcription is disrupted by mutant huntingtin *in vitro* and that Sp1's DNA-binding activity is compromised in early-grade HD brain. Additional factors or mechanisms likely contribute to huntingtin-related gene expression, however, since other genes that contain functional Sp1 response elements are not differentially detected in HD patients or mice. Recent data

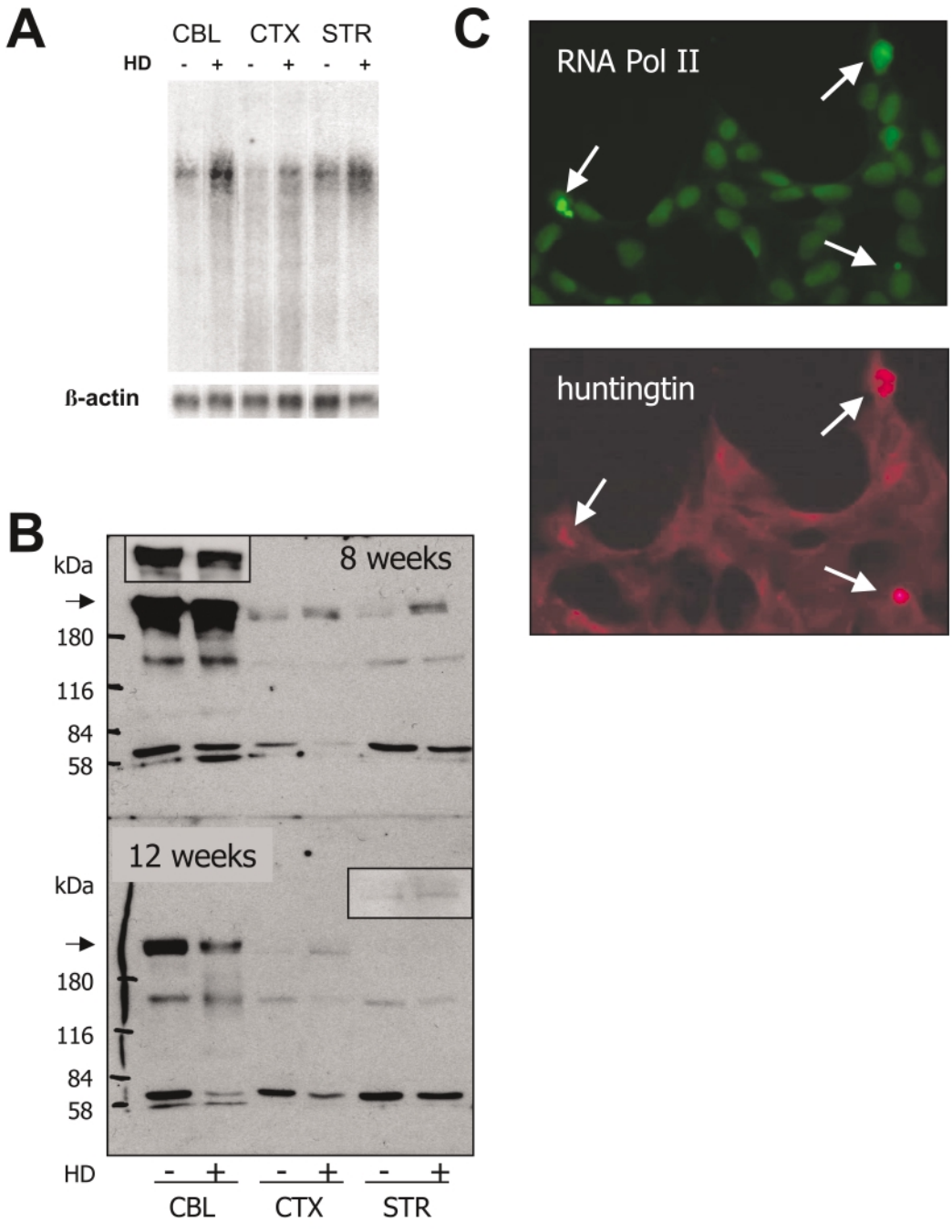

Figure 7. Polyglutamine-related changes in RNA polymerase II large subunit expression. (**A**) Northern blot analysis. Total RNA from R6/2 animals was hybridized to an RNA pol II large subunit cDNA probe. Consistent with microarray analyses (Fig. 2A), increases were observed in R6/2 animals (HD+) in all three brain regions examined [cerebellum (CBL) 439% of control, cerebral cortex (CTX) 156% of control and striatum (STR) 445% of control; $n = 3$ animals of each genotype, one representative sample shown]. Also consistent with microarray measurements, highest levels of the RNA were seen in cerebellum, with less in striatum, and lowest levels in cortex. (**B**) Western blot analysis of RNA polymerase II. Brain lysates from 8-week (top) and 12-week-old (bottom) R6/2 and littermate mice were immunoblotted with antibody to RNA polymerase II (Covance). Arrows indicate the expected 220 kDa immunoreactive band. The insert in the top panel shows a lighter exposure of the 8-week cerebellum lanes and insert in the bottom panel shows a darker exposure of 12-week striatum lanes. Levels of soluble RNA polymerase II protein are increased in the striatum and cortex of R6/2 mice, whereas they are decreased in the cerebellum of these animals.(**C**) Co-localization of RNA polymerase II and huntingtin by immunocytochemistry. Immunostainings for RNA polymerase II (top panel) and huntingtin (bottom panel) were performed in parallel in cells stably transfected with highly truncated mutant huntingtin [N63-82Q (35)]. In this cell line, <15% of cells develop aggregates. RNA polymerase II and huntingtin were detected with a monoclonal antibody to the large subunit of RNA polymerase II (1:100, Covance) and a polyclonal antibody to the 17 amino acids of huntingtin [(36); 1 : 20 000], respectively. As indicated by the arrows, RNA polymerase II was co-localized to the majority of huntingtin-positive aggregates. In highly truncated wild-type huntingtin (N63-18Q) cells (35), RNA polymerase II immunostaining was mainly in the nucleus and huntingtin immunostaining was throughout the cytoplasm, and both stainings were diffuse showing no aggregate formation (data not shown).

Table 3. mRNAs that differ in muscle of R6/2 mice compared to controls

Genbank	Name[a]	Fold change[b]
AI427919	Acyl-Coenzyme A thioesterase 3, mitochondrial	1.3
AI324833	Agrin precursor	2.1
AI450819	Amyloid β(A4) precursor protein	1.3
AI415069	Atopy-related autoantigen CALC	1.3
AI323595	B-cell receptor-associated protein 31	1.7
AI323923	Carbonyl reductase 1	1.6
AI326292	Choline/ethanolamine kinase	1.3
AI450829	Choline/ethanolamine phosphotransferase	1.4
AI385656	Cholinergic receptor, nicotinic, alpha polypeptide 1 (muscle)	3.0
AI450302	DNA-repair protein complementing XP	1.4
AI326934	Fibroblast growth factor receptor 1	1.4
L28177	Growth arrest and DNA-damage-inducible 45 α	1.6
AI452348	Hypothetical protein MGC7670	1.3
AI414367	Keratin complex 2, basic, gene 1	1.3
AI326978	Lactate dehydrogenase 1, A chain	1.5
AI451288	Ornithine decarboxylase, structural	1.3
AI426255	p53-regulated PA26-T2 nuclear protein	2.3
AI428298	Rab6-interacting protein 1	1.6
AI451106	Sacsin	2.6
AI429591	Sialyltransferase 5	1.3
AI450205	Staufen (RNA-binding protein) homolog 2 (*Drosophila*)	1.6
AI413443	Ubiquitin-conjugating enzyme E2G 2	1.3
AI528635	Ubiquitin-conjugating enzyme E2H	1.3
AI448040	Vesicle transport through interactin with t-SNAREs 1b homolog	1.3
Decreased in R6/2 versus control		
M12866	Actin, α1, skeletal muscle	0.4
AI323970	Aldolase 1, A isoform	0.7
AI327146	Aldolase 3, C isoform	0.6
AI413911	Baculoviral IAP repeat-containing 4	0.6
AI528691	B-cell leukemia/lymphoma 3	0.7
AI893653	Chromobox homolog 5 (*Drosophila* HP1a)	0.7
AI413818	Collagenous repeat-containing sequence	0.4
AI324268	Creatine kinase, muscle	0.7
AI426455	Cyclin-dependent kinase 2	0.5
AI323295	DNA-damage-inducible transcript 3	0.7
AI325234	Enolase 3, β muscle	0.6
AI323335	Four and half LIM domains 2	0.7
AI327096	Frequenin homolog (*Drosophila*)	0.6
AI426929	Hormonally upregulated Neu-associated kinase	0.7
AB025099	Kruppel-like factor 5	0.4
AI323629	Low-density lipoprotein receptor	0.7
AI427514	Metallothionein 1	0.6
NM_010866	Myogenic differentiation 1 (MyoD)	0.6
AI324023	Myosin light chain, alkali, fast skeletal muscle	0.5
NM_016754	Myosin light chain, phosphorylatable, fast skeletal muscle	0.6
AI414541	Neurofibromatosis 2-interacting protein	0.6
AI323314	Neuropeptide nociceptin 1	0.7
AI326026	Ornithine decarboxylase antizyme inhibitor	0.7
AI894211	Otoconin 90	0.7
AI325926	Phosphatidylinositol glycan, class F	0.6
AI452258	Phosphodiesterase 4B, cAMP-specific	0.6
AI450876	Pyridoxal (pyridoxine, vitamin B6) kinase	0.7
NM_016676	RAB10, member RAS oncogene family	0.6
AI324640	S-adenosylmethionine decarboxylase 1	0.4
AI326777	Serine (or cysteine) proteinase inhibitor, clade H (heat-shock protein 47),	0.7
AI528769	Transition protein 1	0.6
NM_009405	Troponin 1, skeletal, fast 2	0.7
NM_011620	Troponin T3, skeletal, fast	0.7

Messenger RNAs that were consistently increased (top) or decreased (bottom) in R6/2 gastrocnemius muscle compared with control by cDNA microarray analysis are shown along with the average fold change for each. Differentially expressed genes were identified as previously described using four replicates of each condition (see Materials and Methods).

[a]Table does not include 75 novel sequences (ESTs) that were decreased, nor 34 that were increased.

[b]Refers to fold change in R6/2 muscle compared with control.

from our group and other laboratories suggest that the poly(Q) interactor protein TAFII130 may play also an important role in huntingtin's disruption of transcription at Sp1-regulated promoters (29,32).

This study also demonstrated mRNA changes that are consistent with several other established hypotheses related to poly(Q)-mediated neurodegeneration, including disruption of cAMP response element binding protein (CREB)-binding protein (CBP), retinoid and BDNF activites, altered neurotransmission and cellular metabolism, and induction of stress response systems (16,23–31,40,41,52–55). Numerous genes that are known to be positively regulated through cAMP-responsive or retinoid-response elements were diminished in R6/2 brain, including several genes that were uniformly decreased across multiple brain regions (e.g. preproenkephalin and preprosomatostatin). BDNF levels were decreased in both cerebellum and cerebral cortex, consistent with the hypothesis that reduced trophic support from corticostriatal neurons contributes to striatal medium spiny neuron degeneration (52). The expression of multiple inflammation- and stress-related genes was increased in all regions, and the cerebellum additionally demonstrated evidence of gliosis (GFAP increase) and caspase activation [increased interleukin-1β-converting enzyme (ICE, caspase-1)]. These results are consistent with previous assessments of R6 animals, including pathologic studies showing inflammatory changes in brain (18,56) and mRNA profiling by cDNA array and northern analyses showing increases in cell-death-related mRNAs (56,57). Because northern and western data confirmed positive gene expression changes detected with the use of an error model (33), it should now be possible to generate and test new hypotheses related to HD pathogenesis. With further study, these gene expression changes should aid in the elucidation of the specific molecular mechanisms causing poly(Q)-dependent disruptions in transcription and/or other RNA-processing events.

The R6/2 mouse gene expression profiles provide new targets for analysis in human tissues. Limited comparisons between gene expression changes in R6/2 mice and previous mRNA and protein studies of HD material suggest that R6/2 mice recapitulate many of the earliest biochemical changes observed in HD brain, including decreases in particular neurotransmitter receptors (25,58–60). Ongoing studies will address the extent to which mRNA changes in these mice predict transcriptional abnormalities in human poly(Q) disease.

We tested the hypothesis that neuronal gene expression changes would be mirrored in muscle of R6/2 mice. The functional relationship between the changes in gene expression in nerve and muscle were striking. The tissue-specific forms of creatine kinase, enolase and intermediate filaments were decreased in both brain and muscle, and evidence of cellular stress related to poly(Q) expression was evident in both. The demonstration that poly(Q)-mediated gene and protein level changes can be detected in tissue outside the central nervous system raises the possibility that biomarkers of disease progression will be detectable in skin, muscle, blood or other peripherally accessible tissue. Because current clinical trial endpoints for HD remain unsatisfactory, it is hoped that biomarkers can serve as surrogates in clinical trials, much like reductions of cholesterol levels are used to assess the efficacy of drugs that ultimately reduce cardiac arrest from coronary artery disease (http://www.hdfoundation.org/workshop.htm).

MATERIALS AND METHODS

Animals

R6/2 animals (9) were obtained from Jackson Laboratories (Bar Harbor, ME). Age- and sex-matched groups of mice were sacrificed in parallel at the following ages: 12 ± 1 days ($\sim$2 weeks), 25 ± 2 days ($\sim$4 weeks), 40 ± 2 days ($\sim$6 weeks), 56 ± 4 days ($\sim$8 weeks), 70 ± 4 days ($\sim$10 weeks), and 84 ± 4 days ($\sim$12 weeks). Tissues were dissected rapidly, frozen quickly on dry ice and stored at -80°C until processed.

RNA

RNA was extracted using Tri-Reagent (Sigma-Aldrich, St Louis, MO) according to the manufacturer's instructions. Striatal microarray samples from 2-week-old animals (comprising of total RNA) were additionally purified over RNeasy columns (Qiagen). Poly(A)$^+$ RNA was extracted from 30–80 μg of total RNA using an Oligotex mRNA isolation kit (Qiagen) for other microarray samples.

Microarray analyses

The microarray analyses were conducted using Mu11K A+B GeneChip sets (Affymetrix, Santa Clara, CA) according to the manufacturer's recommendations. RNA samples for 2-week striatal microarray analyses comprised 15 μg of total RNA pooled from four animals (two male and two female). For other microarray samples, poly(A)$^+$ RNA was extracted as described above from total RNA pooled from two to six female R6/2 or wild-type animals. Subsequent cRNA preparation and hybridization was conducted as described in (25). Pairwise comparisons between array samples were conducted using Affymetrix GeneChip Microarray Suite 3.3 or 4.0 software. Data were analyzed using the Difference Call Decision Matrix (61) and as described in (33). Muscle specimens were analyzed on cDNA spotted arrays that were generated in the Fred Hutchinson Cancer Center Microarray Facility. Samples were prepared, hybridized, scanned and analyzed as described previously (62).

Promoter analysis

We searched the Medline database for promoter motifs present in the genes that showed altered expression in the R6/2 transgenic compared with wild-type mice. We found that all genes which had promoter characterization contained putative binding sites for Sp transcription factors (Table 2). Criteria for selection of Sp sites were based on the presence of the consensus sequence (GGGCGGG) within the first 500 bp upstream from the transcription start site. Analysis of more distal transcription factor response elements will be reported separately.

Northern blot analyses

RNA samples (2 μg of total RNA per lane from age- and sex-matched cohorts of animals) were electrophoretically separated

through a 1.2% agarose/3% formaldehyde gel in 1 × MOPS buffer and transferred electrophoretically to GeneScreen II membranes 1 × TAE buffer (NEN Life Sciences, Boston, MA). The resultant blots were hybridized to ^{32}P-labeled cDNA probes in ExpressHyb hybridization medium (Clonetech, Palo Alto, CA) at 68°C for 3–16 h. cDNA probes were labeled by random priming using a Prime-It II kit (Stratagene, Cedar Creek, TX) according to the manufacturer's instructions (high-specific-activity protocol) with [^{32}P]dATP (6000 Ci/mmol; NEN Life Sciences). Blots were washed twice for 15 min with 2 × SSC followed by two sequential high-stringency washes (15 and 30 min) with either 0.2 × SSC + 0.1% SDS (for human cDNA probes: β-actin and hippocalcin) or 0.1 × SSC + 0.1% SDS (for mouse cDNA probes: all others). The β-actin probe (corresponding to bases 658–936 of GenBank accession no. X00351) was a gift from Dr David W. Miller (Massachusetts General Hospital), and the proenkephalin probe (comprising bases 182–655 of GenBank accession no. M13227) was cloned by RT–PCR. Other cDNA probes comprised the following sequence-verified IMAGE clones, obtained from ResGen/Invitrogen: BDNF (1397218), Cathepsin S (596534), CCK (874832), GC-BP (3153027), Hippocalcin (1540054), IGFBP5 (585964), MARCKS (637962), myosin light chain (318218), NAP22 (3971850), neurogranin (445656), NFYC (3325912), PCP4/PEP19 (403628), PDEB1 (557945), PKCδ (1066943), PTZ-17 (ID4160989), RPIILS (1383243), RSE (4017458), SNFK (1229791), somatostatin (480070) and 3CH134 (4235972). Sequence information on these clones is available at www.resgen.com/resources/apps/cdna/index.php3. Autoradiograms were analyzed using a Molecular Dynamics phosphoimager and ImageQuant software v 1.2 (Sunnyvale, CA). To correct for variations in sample loading, hybridization signal for each target mRNA was expressed as a ratio to β-actin signal on the same blot.

Western blotting

Tissue samples from the cerebellum, cortex or striatum were homogenized (1 : 10, w/v) in 0.25 M Tris–HCl, pH 6.8, 1% sodium dodecylsulfate (SDS), 5 mM EGTA, 5 mM EDTA, and 10% glycerol, supplemented with protease inhibitors (Roche). The samples were then sonicated for 15 s and centrifuged for 10 min at 10 000 *g* at 4°C, and the protein concentration of the supernatant was determined using the BCA assay. Samples were diluted to a final concentration of 2 mg/ml in 2 × stop buffer (0.25 M Tris–HCl, pH 6.8, 2% SDS, 25 mM dithiothreitol, 5 mM EGTA, 5 mM EDTA, 10% glycerol and 0.01% bromophenol blue as tracking dye), and incubated in a boiling water bath for 10 min. Then samples were run on 5% SDS–polyacrylamide gels, and then transferred to nitrocellulose. The membranes were blocked for 60 min in Tris-buffered saline/Tween-20 (TBST) (137 mM NaCl, 20 mM Tris–HCl, pH 7.5, 0.1% Tween-20) containing 5% non-fat dried milk. The membranes were incubated overnight at 4°C with RPIILS antibody (Covance) in the blocking buffer. The membranes were then washed three times with TBST and incubated for 2 h with HRP-conjugated secondary antibody and the immunoreactive proteins were detected using a chemiluminescent substrate (ECL, Amersham).

Immunocytochemistry

Cells that express highly truncated mutant huntingtin (35) were seeded on poly-D-lysine-coated cover slips in 24-well plates. Cells were fixed in 90% methanol and 50 mM EGTA, pH 6.0 for 5 min at −20°C (44), incubated for 10 min with 0.2% Triton X-100 in PBS, and rinsed three times with PBS, prior to incubation with 5% bovine serum albumin in PBS for 90 min to reduce the background. Cells were then incubated at room temperature for 90 min with a monoclonal RNA polymerase II antibody (1 : 100, Covance) and a polyclonal N-terminal huntingtin antibody (1 : 20 000) (36) in 5% bovine serum albumin in PBS. Cells were then rinsed with PBS, and incubated for 60 min at room temperature with FITC-conjugated anti-mouse IgG (1 : 100) and Texas Red-conjugated anti-rabbit IgG (1 : 100) in 5% bovine serum albumin in PBS. Coverslips were then washed extensively in PBS and mounted. Cells were viewed using fluorescence microscopy (Zeiss). The digitally stored images were combined and displayed with the accompanying software and Adobe Photoshop 7.0.

ACKNOWLEDGEMENTS

The authors wish to thank Jang-Ho Cha and George Yohrling for critical evaluation of this manuscript, Jeffrey Delrow and the FHCRC Microarray Facility for technical assistance and Sharon Melanson and John Kuster for help in preparing the manuscript. This work was funded by The Hereditary Disease Foundation Cure HD Initiative (R.L.C., J.M.O., D.K. and A.B.Y.), the National Institutes of Health (NS10800 to R.L.C., AG13617 to A.B.Y., NS42157 to J.M.O., NS023174 to D.K., and NS36086 to S.J.T.).

REFERENCES

1. Huntington's Disease Collaborative Research Group (1993) A novel gene containing a trinucleotide repeat that is expanded and unstable on Huntington's disease chromosomes. *Cell*, **72**, 971–983.
2. Young, A.B. (1994) Huntington's disease: lessons from and for molecular neuroscience. *The Neuroscientist*, **Preview issue**, 30–37.
3. Petersen, A., Mani, K., and Brundin, P. (1999) Recent advances on the pathogenesis of Huntington's disease. *Exp. Neurol.*, **157**, 1–18.
4. Strong, T.V., Tagle, D.A., Valdes, J.M., Elmer, L.W., Boehm, K., Swaroop, M., Kaatz, K., Collins, F.S. and Albin, R.L. (1993) Widespread expression of the human and rat Huntington's disease gene in brain and nonneuronal tissues. *Nat. Genet.*, **5**, 259–265.
5. Sharp, A.H., Loev, S.J., Schilling, G., Li, S.H., Li, X.J., Bao, J., Wagster, M.V., Kotzuk, J.A., Steiner, J.P., Lo, A. *et al.* (1995) Widespread expression of Huntington's disease gene (IT15) protein product. *Neuron*, **14**, 1065–1074.
6. Landwehrmeyer, G.B., McNeil, S.M., Dure, L.S., Ge, P., Aizawa, H., Huang, Q., Ambrose, C.M., Duyao, M.P., Bird, E.D., Bonilla, E. *et al.* (1995) Huntington's disease gene: Regional and cellular expression in brain of normal and affected individuals. *Ann. Neurol.*, **37**, 218–230.
7. Paulson, H.L. and Fischbeck, K.H. (1996) Trinucleotide repeats in neurogenetic disorders. *Annu. Rev. Neurosci.*, **19**, 79–107.
8. Ross, C.A., Wood, J.D., Schilling, G., Peters, M.F., Nucifora, F.C.J., Cooper, J.K., Sharp, A.H., Margolis, R.L. and Borchelt, D.R. (1999) Polyglutamine pathogenesis. *Philos. Trans. R. Soc. Lond. B Biol. Sci.*, **354**, 1005–1011.
9. Mangiarini, L., Sathasivam, K., Seller, M., Cozens, B., Harper, A., Hetherington, C., Lawton, M., Trottier, Y., Lehrach, H., Davies, S.W. *et al.* (1996) Exon 1 of the *HD* gene with an expanded CAG repeat is sufficient to cause a progressive neurological phenotype in transgenic mice. *Cell*, **87**, 493–506.

10. Wellington, C.L., Ellerby, L.M., Hackam, A.S., Margolis, R.L., Trifiro, M.A., Singaraja, R., McCutcheon, K., Salvesen, G.S., Propp, S.S., Bromm, M. *et al.* (1998) Caspase cleavage of gene products associated with triplet expansion disorders generates truncated fragments containing the polyglutamine tract. *J. Biol. Chem.*, **273**, 9158–9167.
11. Kim, M., Lee, H.S., LaForet, G., McIntyre, C., Martin, E.J., Chang, P., Kim, T.W., Williams, M., Reddy, P.H., Tagle, D. *et al.* (1999) Mutant huntingtin expression in clonal striatal cells: dissociation of inclusion formation and neuronal survival by caspase inhibition. *J. Neurosci.*, **19**, 964–973.
12. Mende-Mueller, L.M., Toneff, T., Hwang, S.R., Chesselet, M.F. and Hook, V.Y. (2001) Tissue-specific proteolysis of Huntingtin (htt) in human brain: evidence of enhanced levels of N- and C-terminal htt fragments in Huntington's disease striatum. *J. Neurosci.*, **21**, 1830–1837.
13. Kim, Y.J., Yi, Y., Sapp, E., Wang, Y., Cuiffo, B., Kegel, K.B., Qin, Z.H., Aronin, N. and DiFiglia, M. (2001) Caspase 3-cleaved N-terminal fragments of wild-type and mutant huntingtin are present in normal and Huntington's disease brains, associate with membranes, and undergo calpain-dependent proteolysis. *Proc. Natl Acad. Sci. USA*, **98**, 12784–12789.
14. Lione, L.A., Carter, R.J., Hunt, M.J., Bates, G.P., Morton, A.J. and Dunnett, S.B. (1999) Selective discrimination learning impairments in mice expressing the human Huntington's disease mutation. *J. Neurosci.*, **19**, 10428–10437.
15. Carter, R.J., Lione, L.A., Humby, T., Mangiarini, L., Mahal, A., Bates, G.P., Dunnett, S.B. and Morton, A.J. (1999) Characterization of progressive motor deficits in mice transgenic for the human Huntington's disease mutation. *J. Neurosci.*, **19**, 3248–3257.
16. Murphy, K.P., Carter, R.J., Lione, L.A., Mangiarini, L., Mahal, A., Bates, G.P., Dunnett, S.B. and Morton, A.J. (2000) Abnormal synaptic plasticity and impaired spatial cognition in mice transgenic for exon 1 of the human Huntington's disease mutation. *J. Neurosci.*, **20**, 5115–5123.
17. Morton, A.J., Lagan, M.A., Skepper, J.N. and Dunnett, S.B. (2000) Progressive formation of inclusions in the striatum and hippocampus of mice transgenic for the human Huntington's disease mutation. *J. Neurocytol.*, **29**, 679–702.
18. Gutekunst, C.A., Li, S.H., Yi, H., Mulroy, J.S., Kuemmerle, S., Jones, R., Rye, D., Ferrante, R.J., Hersch, S.M. and Li, X.J. (1999) Nuclear and neuropil aggregates in Huntington's disease: relationship to neuropathology. *J. Neurosci.*, **19**, 2522–2534.
19. Turmaine, M., Raza, A., Mahal, A., Mangiarini, L., Bates, G.P. and Davies, S.W. (2000) Nonapoptotic neurodegeneration in a transgenic mouse model of Huntington's disease. *Proc. Natl Acad. Sci. USA*, **97**, 8093–8097.
20. Vonsattel, J.P., Myers, R.H., Stevens, T.J., Ferrante, R.J., Bird, E.D. and Richardson, E.P. (1985) Neuropathological classification of Huntington's disease. *J. Neuropathol. Exp. Neurol.*, **44**, 559–577.
21. Vonsattel, J.P. and DiFiglia, M. (1998) Huntington disease. *J. Neuropathol. Exp Neurol.*, **57**, 369–384.
22. Sathasivam, K., Hobbs, C., Turmaine, M., Mangiarini, L., Mahal, A., Bertaux, F., Wanker, E.E., Doherty, P., Davies, S.W. and Bates, G.P. (1999) Formation of polyglutamine inclusions in non-CNS tissue. *Hum. Mol. Genet.*, **8**, 813–822.
23. Hurlbert, M.S., Zhou, W., Wasmeier, C., Kaddis, F.G., Hutton, J.C. and Freed, C.R. (1999) Mice transgenic for an expanded CAG repeat in the Huntington's disease gene develop diabetes. *Diabetes*, **48**, 649–651.
24. Fain, J.N., Del Mar, N.A., Meade, C.A., Reiner, A. and Goldowitz, D. (2001) Abnormalities in the functioning of adipocytes from R6/2 mice that are transgenic for the Huntington's disease mutation. *Hum. Mol. Genet.*, **10**, 145–152.
25. Luthi-Carter, R., Strand, A., Peters, N.L., Solano, S.M., Hollingsworth, Z.R., Menon, A.S., Frey, A.S., Spektor, B.S., Penney, E.B., Schilling, G. *et al.* (2000) Decreased expression of striatal signaling genes in a mouse model of Huntington's disease. *Hum. Mol. Genet.*, **9**, 1259–1271.
26. Steffan, J.S., Kazantsev, A., Spasic-Boskovic, O., Greenwald, M., Zhu, Y.Z., Gohler, H., Wanker, E.E., Bates, G.P., Housman, D.E. and Thompson, L.M. (2000) The Huntington's disease protein interacts with p53 and CREB-binding protein and represses transcription. *Proc. Natl Acad. Sci.USA*, **97**, 6763–6768.
27. McCampbell, A., Taylor, J.P., Taye, A.A., Robitschek, J., Li, M., Walcott, J., Merry, D., Chai, Y., Paulson, H., Sobue, G. *et al.* (2000) CREB-binding protein sequestration by expanded polyglutamine. *Hum. Mol. Genet.*, **9**, 2197–2202.
28. Nucifora, F.C., Jr, Sasaki, M., Peters, M.F., Huang, H., Cooper, J.K., Yamada, M., Takahashi, H., Tsuji, S., Troncoso, J., Dawson, V.L. *et al.* (2001) Interference by huntingtin and atrophin-1 with cbp-mediated transcription leading to cellular toxicity. *Science*, **291**, 2423–2428.
29. Shimohata, T., Nakajima, T., Yamada, M., Uchida, C., Onodera, O., Naruse, S., Kimura, T., Koide, R., Nozaki, K., Sano, Y. *et al.* (2000) Expanded polyglutamine stretches interact with TAFII130, interfering with CREB-dependent transcription. *Nat Genet.*, **26**, 29–36.
30. Steffan, J.S., Bodai, L., Pallos, J., Poelman, M., McCampbell, A., Apostol, B.L., Kazantsev, A., Schmidt, E., Zhu, Y.Z., Greenwald, M. *et al.* (2001) Histone deacetylase inhibitors arrest polyglutamine-dependent neurodegeneration in *Drosophila. Nature*, **413**, 739–743.
31. Wyttenbach, A., Swartz, J., Kita, H., Thykjaer, T., Carmichael, J., Bradley, J., Brown, R., Maxwell, M., Schapira, A., Orntoft, T.F. *et al.* (2001) Polyglutamine expansions cause decreased CRE-mediated transcription and early gene expression changes prior to cell death in an inducible cell model of Huntington's disease. *Hum. Mol. Genet.*, **10**, 1829–1845.
32. Dunah, A.W., Jeong, H., Griffin, A., Kim, Y.M., Standaert, D.G., Hersch, S.M., Mouradian, M.M., Young, A.B., Tanese, N. and Krainc, D. (2002) Sp1 and TAFII130 transcriptional activity disrupted in early huntington's disease. *Science*, **296**, 2238–2243.
33. Strand, A.D., Olson, J.M. and Kooperberg, C. (2002) Estimating the statistical significance of gene expression changes observed with oligonucleotide arrays. *Hum. Mol. Genet.*, in press.
34. Ideker, T., Thorsson, V., Ranish, J.A., Christmas, R., Buhler, J., Eng. J.K., Bumgarner, R., Goodlett, D.R., Aebersold, R. and Hood, L. (2001) Integrated genomic and proteomic analyses of a systematically perturbed metabolic network. *Science*, **292**, 929–934.
35. Chun, W., Lesort, M., Tucholski, J., Ross, C.A. and Johnson, G.V. (2001) Tissue transglutaminase does not contribute to the formation of mutant huntingtin aggregates. *J. Cell Biol.*, **153**, 25–34.
36. Lin, C.H., Tallaksen-Greene, S., Chien, W.M., Cearley, J.A., Jackson, W.S., Crouse, A.B., Ren, S., Li, X.J., Albin, R.L. and Detloff, P.J. (2001) Neurological abnormalities in a knock-in mouse model of Huntington's disease. *Hum Mol Genet.*, **10**, 137–144.
37. Myers, R.H., Marans, K.S. and MacDonald, M.E. (1998) Huntington's disease. In Wells, R.D. and Warren, S.T. (eds), *Genetic Instabilities and Hereditary Neurological Diseases,* Academic Press, San Diego, pp. 301–323.
38. Luthi-Carter, R., Strand, A.D., Hanson, S.A., Kooperberg, C., Schilling, G., La Spada, A.R., Merry, D., Young, A.B., Ross, C.A., Borchelt, D.R. and Olson, J.M. (2002) Polyglutamine and transcription: gene expression changes shared by DRPLA and Huntington's disease mouse models reveal context-independent effects. *Hum. Mol. Genet.*, **11**, 1927–1937.
39. Chan, E.Y.W., Luthi-Carter, R., Strand, A., Solano, S.M., Hanson, S.A., Kooperberg, C., Chase, K.O., Young, A.B., Leavitt, B.R., Cha, J.-H.J. *et al.* (2002) Increased huntingtin protein length reduces the number of polyglutamine-induced gene expression changes in mouse models of Huntington's disease. *Hum. Mol. Genet.*, **11**, 1939–1951.
40. Hughes, R.E., Lo, R.S., Davis, C., Strand, A.D., Neal, C.L., Olson, J.M. and Fields, S. (2001) Altered transcription in yeast expressing expanded polyglutamine. *Proc. Natl Acad Sci. USA*, **98**, 13201–13206.
41. Sipione, S., Rigamonti, D., Valenza, M., Zuccato, C., Conti, L., Pritchard, J., Kooperberg, C., Olson, J. and Cattaneo, E. (2002) Early transcriptional profiles in huntingtin-inducible striatal cells by microarray analyses. *Hum. Mol. Genet.*, **11**, 1953–1965.
42. Davies, S.W., Turmaine, M., Cozens, B.A., DiFiglia, M., Sharp, A.H., Ross, C.A., Scherzinger, E., Wanker, E.E., Mangiarini, L. and Bates, G.P. (1997) Formation of neuronal intranuclear inclusions underlies the neurological dysfunction in mice transgenic for the HD mutation. *Cell*, **90**, 537–548.
43. Scherzinger, E., Lurz, R., Turmaine, M., Mangiarini, L., Hollenbach, B., Hasenbank, R., Bates, G.P., Davies, S.W., Lehrach, H. and Wanker, E.E. (1997) Huntingtin-encoded polyglutamine expansions form amyloid-like protein aggregates *in vitro* and *in vivo. Cell,* **90**, 549–558.
44. Kazantsev, A., Preisinger, E., Dranovsky, A., Goldgaber, D. and Housman, D. (1999) Insoluble detergent-resistant aggregates form between pathological and nonpathological lengths of polyglutamine in mammalian cells. *Proc. Natl Acad. Sci. USA*, **96**, 11404–11409.
45. Boutell, J.M., Thomas, P., Neal, J.W., Weston, V.J., Duce, J., Harper, P.S. and Jones, A.L. (1999) Aberrant interactions of transcriptional repressor

proteins with the Huntington's disease gene product, huntingtin. *Hum. Mol. Genet.*, **8**, 1647–1655.
46. McCampbell, A. and Fischbeck, K.H. (2001) Polyglutamine and CBP: fatal attraction? *Nat. Med.*, **7**, 528–530.
47. Cha, J.H. (2000) Transcriptional dysregulation in Huntington's disease. *Trends Neurosci.*, **23**, 387–392.
48. Shimohata, T., Onodera, O. and Tsuji, S. (2001) Expanded polyglutamine stretches lead to aberrant transcriptional regulation in polyglutamine diseases. *Hum. Cell*, **14**, 17–25.
49. McCampbell, A., Taye, A.A., Whitty, L., Penney, E., Steffan, J.S. and Fischbeck, K.H. (2001) Histone deacetylase inhibitors reduce polyglutamine toxicity. *Proc. Natl Acad. Sci. USA*, **98**, 15 179–15 184.
50. Bates, G.P. (2001) Huntington's disease. Exploiting expression. *Nature*, **413**, 691 and 693–694.
51. Li, S.H., Cheng, A.L., Zhou, H., Lam, S., Rao, M., Li, H. and Li, X.J. (2002) Interaction of Huntington disease protein with transcriptional activator Sp1. *Mol. Cell. Biol.*, **22**, 1277–1287.
52. Zuccato, C., Ciammola, A., Rigamonti, D., Leavitt, B.R., Goffredo, D., Conti, L., MacDonald, M.E., Friedlander, R.M., Silani, V., Hayden, M.R. *et al.* (2001) Loss of huntingtin-mediated BDNF gene transcription in Huntington's disease. *Science*, **293**, 493–498.
53. Chai, Y., Koppenhafer, S.L., Bonini, N.M. and Paulson, H.L. (1999) Analysis of the role of heat shock protein (Hsp) molecular chaperones in polyglutamine disease. *J. Neurosci.*, **19**, 10338–10347.
54. Kegel, K.B., Kim, M., Sapp, E., McIntyre, C., Castano, J.G., Aronin, N. and DiFiglia, M. (2000) Huntingtin expression stimulates endosomal–lysosomal activity, endosome tubulation, and autophagy. *J. Neurosci.*, **20**, 7268–7278.
55. Trettel, F., Rigamonti, D., Hilditch-Maguire, P., Wheeler, V.C., Sharp, A.H., Persichetti, F., Cattaneo, E. and MacDonald, M.E. (2000) Dominant phenotypes produced by the HD mutation in STHdh(Q111) striatal cells. *Hum. Mol. Genet.*, **9**, 2799–2809.
56. Ona, V.O., Li, M., Vonsattel, J.P., Andrews, L.J., Khan, S.Q., Chung, W.M., Frey, A.S., Menon, A.S., Li, X.J., Stieg, P.E. *et al.* (1999) Inhibition of caspase-1 slows disease progression in a mouse model of Huntington's disease. *Nature*, **399**, 263–267.
57. Iannicola, C., Moreno, S., Oliverio, S., Nardacci, R., Ciofi-Luzzatto A., and Piacentini, M. (2000) Early alterations in gene expression and cell morphology in a mouse model of Huntington's disease. *J. Neurochem.*, **75**, 830–839.
58. Weeks, R.A., Piccini, P., Harding, A.E. and Brooks, D.J. (1996) Striatal D1 and D2 dopamine receptor loss in asymptomatic mutation carriers of Huntington's disease. *Ann. Neurol.*, **40**, 49–54.
59. Cha, J.H., Kosinski, C.M., Kerner, J.A., Alsdorf, S.A., Mangiarini, L., Davies, S.W., Penney, J.B., Bates, G.P. and Young, A.B. (1998) Altered brain neurotransmitter receptors in transgenic mice expressing a portion of an abnormal human Huntington disease gene. *Proc. Natl Acad. Sci. USA*, **95**, 6480–6485.
60. Glass, M., Dragunow, M. and Faull, R.L. (2000) The pattern of neurodegeneration in Huntington's disease: a comparative study of cannabinoid, dopamine, adenosine and GABA(A) receptor alterations in the human basal ganglia in Huntington's disease. *Neuroscience*, **97**, 505–519.
61. Lipshutz, R.J., Fodor, S.P., Gingeras, T.R. and Lockhart, D.J. (1999) High density synthetic oligonucleotide arrays. *Nat Genet.*, **21**, 20–24.
62. Bergstrom, D.A., Penn, B.H., Strand, A., Perry, R.L., Rudnicki, M.A. and Tapscott, S.J. (2002) Promoter-specific regulation of MyoD binding and signal transduction cooperate to pattern gene expression. *Mol. Cell*, **9**, 587–600.